THE JOURNAL OF PHYSICAL CHEMISTRY A

Article

Applications of a *Bis*-Urea Phenylethynylene Self-Assembled Nanoreactor for [2+2] Photodimerizations.

Sandipan Dawn, Sahan R. Salpage, Brent A. Koscher, Andreas Bick, Arief C Wibowo, Perry J. Pellechia, and Linda S. Shimizu

J. Phys. Chem. A, **Just Accepted Manuscript** • DOI: 10.1021/jp505304n • Publication Date (Web): 11 Jul 2014

Just Accepted

The Journal of Physical Chemistry A is published by the American Chemical Society. 1155 Sixteenth Street N.W., Washington, DC 20036

Applications of a *Bis*-Urea Phenylethynylene Self-Assembled Nanoreactor for [2+2] Photodimerizations.

Sandipan Dawn,[†#] Sahan R. Salpage,[†#] Brent A. Koscher,[†] Andreas Bick,[‡] Arief C. Wibowo,[†+] Perry J. Pellechia,[†] and Linda S. Shimizu[†]*

[†]Department of Chemistry and Biochemistry, University of South Carolina, Columbia, SC 29208, USA

[‡]Scienomics SARL, 16 rue de l'Arcade, 75008 Paris France

KEYWORDS Microporous environment, cyclic bis-urea macrocycles, Grand Canonical Molecular Modeling, [2+2]-photocycloadditions, coumarins

Supporting Information Placeholder

ABSTRACT: Confined environments can be used to alter the selectivity of a reaction by influencing the organization of the reactants, altering the mobility of trapped molecules, facilitating one reaction pathway or selectively stabilizing the products. This manuscript utilizes a series of potentially photoreactive guests to interrogate the utility of the one-dimensional nanochannels of a porous host to absorb and to facilitate the reaction of encapsulated guests. The host is a columnar self-assembled phenylethynylene *bis*-urea macrocycle, which absorbs guests including coumarin, 6-methyl coumarin, 7-methyl coumarin, 7-methoxy coumarin, acenaphthylene, *cis*-stilbene, *trans*-stilbene and *trans*-β-methyl styrene to afford crystalline inclusion complexes. We examine the structure of the host:guest complexes using powder X-ray diffraction, which suggests that they are well-ordered highly crystalline materials. Investigations using solid state cross-polarized magic angle spinning $^{13}C\{^{1}H\}$CP-MAS NMR spectroscopy indicate that the guests are mobile relative to the host. Upon UV-irradiation, we observed selective photodimerization reactions for coumarin, 6-methyl coumarin, 7-methyl coumarin, and acenaphthylene, while the other substrates were unreactive even under prolonged UV-irradiation. Grand Canonical Monte Carlo simulations suggest that the reactive guests were close paired and preorganized in configurations that facilitate the photodimerization with high selectivity while the unreactive guests did not exhibit similar close pairing. A greater understanding of the factors that control diffusion and reaction in confinement could lead to the development of better catalysts.

Keywords: Bis-urea macrocycles, Grand Canonical Monte Carlo simulations, coumarins, acenaphthylene, [2+2] photocycloadditions, solid state cross-polarized magic angle spinning NMR spectroscopy.

INTRODUCTION

Confined environments can potentially be used to modulate the chemical reactivity of encapsulated guests with the goal of controlling their reactions and inducing selectivity.[1,2] A host that provides a confinement environment for reaction is popularly termed a 'nanoreactor'.[3] A few of the chemical processes that are facilitated within nanoreactors include unimolecular aza-cope rearrangements,[4,5] bimolecular Diels-Alder reactions,[6,7] oxidations,[8,9] and [2+2] photodimerization reactions.[10,11] They have also been used to stabilize reactive substances[12,13] and intermediates.[14,15,16,17] In many cases, the encapsulated guest molecules interact both with the walls of the host and with each other and can be constrained to adopt a particular orientation within these small spaces.[18] The interactions that orient these guests depend on their chemical nature and on the specific structure of the hosts and occur between the host and guests and between neighboring guests. The strength, directionality and reversibility of these interactions guide the structure of these complexes both before and after reaction. A greater understanding of the factors that control reaction in confinement could lead to the development of better catalysts.

Recently, we reported *bis*-urea phenylethynylene macrocycle **1** (Figure 1a), which assembles into columnar structures from several solvents.[19] These columns pack together to afford micron sized porous crystals with nanometer range channels. The crystallization solvent could be removed by heating, and the empty host displayed permanent porosity by gas adsorption and showed a surface area of ~ 350 m^2/g. From the X-

ray structure of host **1**•nitrobenzene (Figure 1c), one can see that the accessible columns are lined with ureas and aryl groups. This manuscript explores the absorption of a series of guests (Figure 1b), which have a propensity to undergo light driven reactions, into these porous crystals. We examine the structure of these crystalline inclusion complexes by both solid-state and computational studies using Grand Canonical Monte Carlo (GCMC) simulations. The simulations were able to differentiate between the guests that undergo reactions within the columnar channels (coumarin, 6-methyl coumarin, 7-methyl coumarin and acenaphthylene) versus guests that were unreactive within the channels (7-methoxy coumarin, stilbenes and styrene). Guests that were reactive were bound in close proximity within the channels in relative geometries that were close to those required for photoreaction. In contrast, unreactive guests were not close paired but were randomly distributed within the tubes and displayed few contacts with neighboring guests.

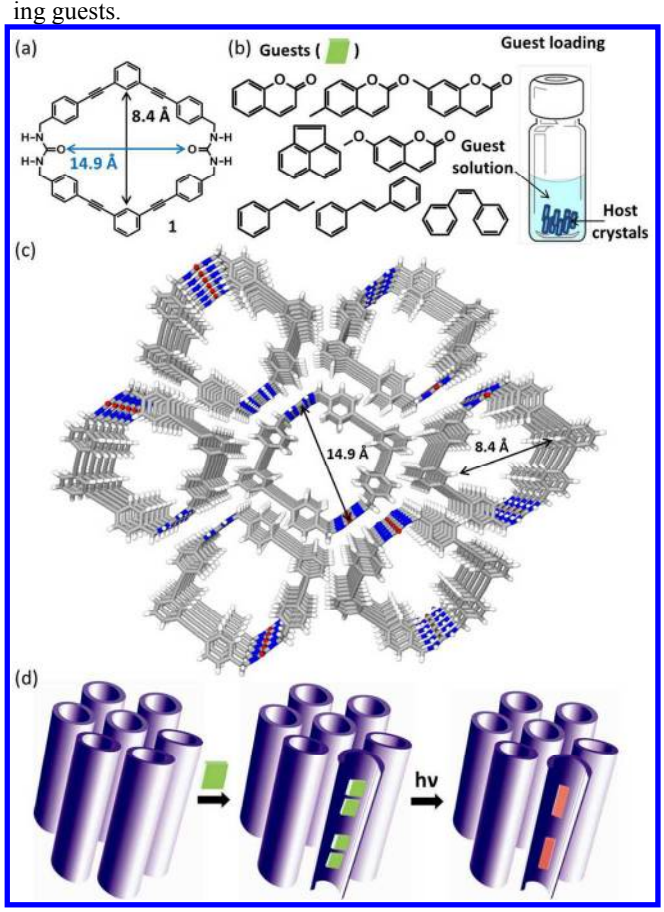

Figure 1. Columnar assembled host **1** forms porous crystals with accessible channels for binding guests. a). Structure of macrocycle **1**. b). Guests that load into the crystals from solution. c). View from the X-ray structure of **1**•nitrobenzene shows the packing of aligned one-dimensional channels (disorder solvent removed for clarity). d). Schematic of guest loading and subsequent reaction in the simple tubular channels.

The uptake of reactants into open cavities, pores, and channels or the formation of co-crystals results in complexes where the guests display restricted motion, altered mobility or preorganization that can lead to selective conversions or facilitate pathways and products that are not observed in solution.[20] It is the organization of reactants within this confined space or 'reaction cavity'[21,22,23] which are key to understanding the product distribution for a given transformation. Imagination and synthetic accessibility are a few of the limits when it comes to designing a confined space. The confined space may consist of a discrete cavity or pore in a small molecular host in solution such as cyclodextrins,[24] calixarenes,[25] or cucurbiturils.[26] It could be the larger interiors of small to medium sized assembled structures, such as cavitands[27] or Gibbs Octa acids,[28] as well as nanoscale structures such as coordination spheres,[1] proteins and polymers.[29] Reaction cavities are not limited to soluble hosts in solution, but can also be voids in solids or templated and preorganized asssemblies in co-crystals such as the innovative work from Toda,[30] and MacGillivray.[31]

In comparison, host **1** presents a high density of aligned, one-dimensional channels with ~ 9 Å diameter (Figure 1a), which are accessible to guests. Previously, we have loaded coumarin into these channels.[19] Figure 2a illustrates a view of half of the channel from the X-ray structure to highlight the aryl, ethynylene, and urea groups that line the channels. Our hypothesis is the ureas are unable to participate in further hydrogen bonding interactions with the guests as the three centered urea hydrogen bonding motif is used to construct the columnar framework. Molecular modeling with Scienomics MAPS[32] of the host **1**•coumarin complex suggests that the encapsulated guests form aryl stacking and dipole interactions between the coumarin and the phenyls that line the channel as well as dipole interactions between the coumarin oxygen and the urea groups (Figure 2b).

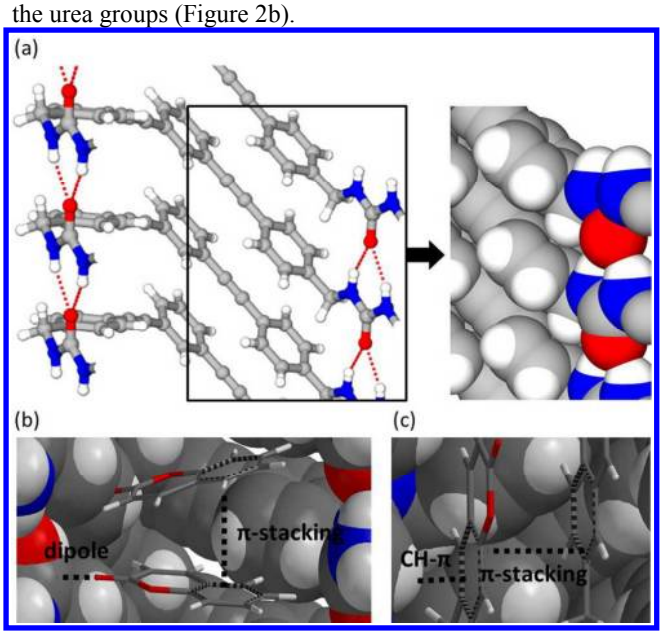

Figure 2. Views of host **1** and host **1** complexes: a) View of half of the channel illustrating the aryl, ethynyl and hydrogen bonded urea groups that line the interior. b) Molecular models of the host **1**•coumarin inclusion complexes generated with Scienomic's MAPS[32] illustrate the aryl stacking interactions that can occur between the neighboring coumarins as well as the dipole-dipole interactions between coumarin and the column walls. c) Aryl stacking and CH-π aid in binding of 6-methyl coumarin in the channel's interior.

We chose to test seven different guests: those that undergo [2+2] photocycloadditions (6-methyl and 7-methyl coumarin, 7-methoxy coumarin and acenaphthylene) and three that undergo photo-isomerization reactions (*cis*- and *trans*-stilbene and *trans*-β-methyl styrene) (Table 1). In addition, *trans*-β-methyl styrene can also act as a probe to test if the host itself can be a photosensitizer, as it will only undergo isomerization

in the presence of a medium energy sensitizer, such as chrysene or 1-acetylnaphthalene.[33] We evaluated the absorption of these guests by host **1** and characterized the structure of their inclusion complexes by solid-state methods. We then investigated if these encapsulated guests would undergo photochemical reactions upon UV-irradiation. Some of the guests underwent photochemical reactions within the solid complex in moderate to good yields with high selectivity while others were unreactive within these solid inclusion complexes. Molecular modeling studies allowed us to probe the fit of the guests inside the channel of the host. These studies were directed at understanding the following questions: Are certain orientations of the guest molecules stabilized by the confinement? Are they appropriately oriented to undergo photodimerization or photoisomerization reaction?

EXPERIMENTAL AND COMPUTATIONAL DETAILS

Sample Preparation. Macrocycle **1** was prepared as previously described.[19] Crystals were obtained by slow cooling a DMSO solution of **1** (50 mg/ 10 mL) from 140 °C at 1 °C / h. Small needle crystals of **1**•DMSO were observed in 2-3 days and displayed a 1:2 host **1**:DMSO stoichiometry. Host **1** was obtained by heating the **1**•DMSO crystals using thermogravimetric analysis (TGA). Freshly obtained crystals (15 mg) were heated from 25 to 170 °C (4 °C/min). A two-step desorption curve was observed with a total weight loss of 18.3%, corresponding to removal of the DMSO. The crystals were cooled under helium (g) and used directly for loading experiments.

Guest loading. Guests were loaded in the empty host by two methods. A) The crystalline host was soaked in solution of the guest in a suitable solvent (CH_3CN or hexanes) for 0-24 h. B) The host was immersed directly in the liquid guest. For method A typical loading experiments were carried out on samples of host **1** (5-50 mg) by soaking in guest solutions (0.1 mM in CH_3CN for most guests or 0.5 mM in hexanes at 35 °C for 7-methoxy coumarin. As these guests all contain UV chromophores, their depletion from solution was followed by absorption spectroscopy until the absorbance reached a plateau, suggesting that equilibrium had been obtained. The loading ratios were then calculated through comparison to Lambert-Beer plots of known concentrations of the guest. Loading experiments were carried out on different batches and sizes of host **1** crystals and gave similar binding ratios. For method B host **1** (30 mg) was added to the pure liquid guest (10 mL) in a scintillation vial and kept undisturbed for equilibration (12 h). After filtration, the complexes were air dried (6 h) and analyzed by TGA. Two guests *cis*-stilbene and *trans*-β-methyl styrene were loaded by this method as they showed no loading by method A.

Photoreactions. Each host **1**•guest complex (30 mg) was placed in a Norell S-5-500-7 NMR tubes (with 100% transmittance up to 400 nm). Samples of the pure guests (30 mg) were also used as controls. The samples were UV-irradiated at room temperature under argon atmosphere using a Hanovia 450 W medium pressure mercury arc lamp for between 0-96 h. Products were extracted into deuterated solvent for analysis. Additionally, the solid-complexes (2-3 mg) were also directly dissolved in DMSO-d_6 and analyzed by ^{1}H NMR spectroscopy to confirm that the products could be fully removed from the crystals.

Powder X-ray Diffraction (PXRD). The powder X-ray diffraction (PXRD) data were collected on a Rigaku Dmax-2100 & 2200 powder X-ray diffractometers using a Bragg-Brentano geometry with CuKα radiation. The step scans covered the angular range 2-40° 2θ in steps of 0.05°.

Solid-state cross-polarized magic angle spinning ^{13}C{^{1}H}CP-MAS NMR spectra. Solid state ^{13}C CP-MAS spectra were collected on a Bruker Avance III-HD 500 MHz spectrometer fitted with a 1.9 mm MAS probe. The spectra were collected at ambient temperature with sample rotation rate of 20 kHz. 1.5 ms contact time with linear ramping on the ^{1}H channel and 62.5 kHz field on the ^{13}C channel were used for cross polarization. ^{1}H dipolar decoupling was performed with SPINAL64 modulation and 145 kHz field strength. Free induction decays were collected with a 27 ms acquisition time over a 300 ppm spectra width with a relaxation delay of 1.5 s. In comparison, spectra from prior reports were acquired using double resonant Doty Scientific XC 4 mm MAS probe.[19] TPPM modulated dipolar decoupling with 61 kHz field strength was applied during data acquisition. One second equilibration delay was used between each transient. Spinning speed of 8 kHz and TOSS side-band suppression was used for all measurements. Ramped cross polarization was used.

Thermogravimetric analysis (TGA). TGA guest desorption studies were carried out on 5-10 mg of absorbed sample using TA Instruments SDT-Q600 simultaneous DTA-TGA at a heating rate of 4ºC/min from 25 to 170 ºC under helium.

Computational studies. Computational studies were performed using the Monte Carlo for Complex Chemical Systems (MCCCS) Towhee plug-in built into Scienomics' Materials Processes and Simulations (MAPS) platform.[32] First, amorphous guest systems were built using the Amorphous Builder plug-in within MAPS, and the chemical potentials of guests were calculated *via* a 1 x 10^4 step canonical MC simulation with MCCCS Towhee for systems contain 100 guest molecules. The Dreiding force field[34] was applied to all our simulated systems. Next, we generated a simulation cell by importing the atomic coordinates from the X-ray structure of host **1**•nitrobenzene.[19] The coordinates of the guests were removed to create a periodic simulation cell. (Supporting Information, MC moves and probabilities tabulated). The calculations of host **1**•guest complexes were performed using previously obtained guest chemical potential values. All calculations were conducted via GCMC simulations for 1x10^6 steps where the chemical potential (μ) of the corresponding guest was kept constant and the system was maintained at standard ambient constant temperature (t, 298.15K) and constant volume (V).

RESULTS AND DISCUSSION

In our previous work, we reported the X-ray structure of host **1** from DMSO/nitrobenzene (host **1**•nitrobenzene) and demonstrated that the structure of the host is similar when crystallized from DMSO (host **1**•DMSO).[19] The encapsulated solvent can be removed from the channels of each of these complexes to give the same empty host as indicated by their identical PXRD pattern. The channels can subsequently be reloaded with either solvent or alternatively with a different guest. Figure 1c highlights the channel of this host, which is approximately ~ 9 Å in diameter. The channel is lined with polar urea groups that are occupied in the hydrogen bonding scheme that runs along the channel's frame (Figure 2a). Aryl and ethynyl groups also line the channel. This manuscript investigates the loading of a series of guests within the channel of these pores through both experimental and computa-

tional methods. These guests were chosen for their similarity in polarity to coumarin. Furthermore, these guests were selected based on their size, shape and potential photoreactivity.

Host **1** was synthesized and characterized by ^{1}H and ^{13}C NMR in DMSO-d_6 solution. After crystallization from DMSO, the host **1**•DMSO solvate was further characterized by PXRD, solid-state NMR and TGA (Supporting Information). The channel of the newly recrystallized material was filled with DMSO solvent, which needed to be removed before a new guest could be loaded. Figure 3 illustrates the process of desorption and adsorption of guests schematically. Host **1**•DMSO crystals show a two step curve (TGA 1) with corresponding weight loss of 9.1% between 30 and 80 °C and an 4.9% weight loss between 80 and 130 °C. Previous work with the 'empty' host demonstrated a type 1 gas adsorption isotherm with CO_2 (g) with an apparent surface area of 349 m^2/g at 273 K.[19] For absorption of new guests, the 'empty' host obtained by TGA was cooled under helium gas then transferred directly to a solution containing guest (method A) or to an aliquot of liquid guest (method B). The channels are guest accessible and the crystals could be reused many times. For example, after removal of the DMSO (Figure 3, TGA 1) the crystals were treated with DMSO (method B). TGA 2 (Figure 3) shows a nearly identical two step desorption curve with a weight loss of 8.3% between 30 and 80 °C and an 5.2% weight loss between 80 and 130 °C. These empty crystals were reloaded again with DMSO and also showed a similar two step desorption curve (Figure 3, TGA 3). Different batches and sizes of crystals showed reversible absorption with similar host:DMSO ratios. These experiments demonstrate that guests can be reversibly bound by host **1** and suggest that they are bound in discrete binding sites.

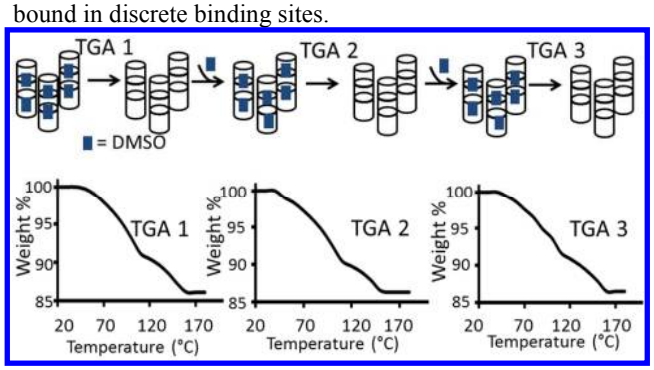

Figure 3. Reversible absorption/desorption of guests: (Top) Schematic depicting of desorption and reabsorption of DMSO. (Bottom) Three successive cycles showing TGA desorption for host **1**•DMSO.

As the channel of host **1** is much larger than our earlier hosts, we focused on guests that were similar or larger in volume than the parent coumarin. A series of coumarins (coumarin, 6-methyl coumarin, 7-methyl coumarin, and 7-methoxy coumarin) were loaded into the porous host by method A. Loading experiments were carried out a minimum of 3 times on different batches and sizes of host **1** crystals and gave similar binding ratios. The reproducibility of the loading ratio suggests that guests are absorbed into discrete binding sites and are not merely surface absorbed. For example, host **1** (30 mg) was soaked in a solution of 6-methyl coumarin (0.1 mM CH_3CN) for 0-12 h. The depletion of 6-methyl coumarin from solution was monitored by absorbance spectroscopy at 273 nm (Figure 4a). The absorbance reached a plateau by 3 h, suggesting that we reached an equilibrium and no further 6-methyl coumarin was absorbed. Assuming that the loss of guest from solution corresponds to the binding of guest in host **1**, we compared the final absorbance to Lambert-Beer plots of known concentrations of the guest in CH_3CN (Supporting Information). This gave calculated host:guest ratio of 1:1, and an average ratio of 1:1.0 from 5 loading experiments. Coumarin (0.1 mM CH_3CN), 7-methyl coumarin (0.1 mM CH_3CN) and 7-methoxy coumarin (0.5 mM in hexanes at 35 °C) were loaded similarly. Figure 4a shows the decrease in absorbance versus time as each of these coumarin guests are separately equilibrated with fresh crystalline host **1**. The guests were monitored at slightly different wavelengths depending on their absorption maxima. Comparison of the absorbance at the plateau to a Lambert-Beer plot (Supporting Information) gave a calculated host:guest ratio for a specific guest. Table 1 compares the guest structure, dimensions, volume and polarity with the observed host:guest binding ratio. For coumarin derivatives, the smallest coumarin, displayed the highest binding ratio (1:1.4) while the largest derivative 7-methoxy coumarin showed the smallest binding ratio (1:0.5). The 6- and 7-methyl derivatives had similar sizes and gave similar ratios (~ 1:1). Overall, the coumarin and methyl coumarins have similar polarities and their size appears to be the primary determinant in their uptake into the channels of the host. In the case of 7-methoxy coumarin, polarity appears to play a greater role in determining guest absorption. This coumarin derivative is more polar than 7-methyl coumarin (7.1 versus 5.8 D) but only slightly larger and was bound in the lowest ratio 1:0.5.

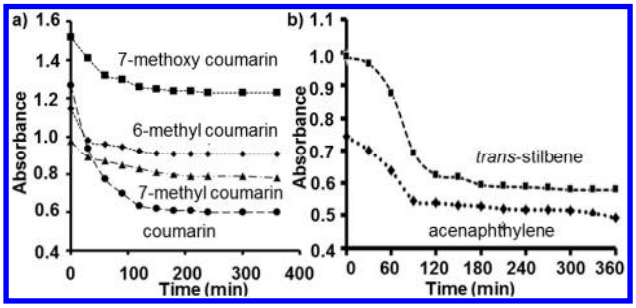

Figure 4. Absorption of guests by host **1**: a) Coumarin derivatives: The depletion of 6-methyl coumarin from solution (0.1 mM in CH_3CN) monitored at 273 nm. The depletion of 7-methyl coumarin from solution (0.1 mM in CH_3CN) monitored at 276 nm. The depletion of 7-methoxy coumarin (0.5 mM in hexanes) was monitored at 315 nm. The depletion of coumarin was reported previously.[19] b) The depletion of acenaphthylene from solution (0.1 mM in CH_3CN) monitored at 322 nm. The depletion of *trans*-stilbene (0.1 mM in CH_3CN) monitored at 295 nm.

As Figures 1 and 2 illustrate, the interior channel of the host is lined with aromatic groups and polar urea groups that provide a suitable space to absorb the polar coumarin derivatives of complementary size. We next investigated aromatic hydrocarbons, which are less polar than the coumarins but still offer aryl surfaces that may form aryl stacking interactions with the sides of the channels. Acenaphthylene, *cis*- and *trans*-stilbene and *trans*-β-methyl styrene are not polar based on their dielectric constants, but contain a quadrupole and are polarizable according the π* scale.[35] Method A was used to load acenaphthylene (0.1 mM in CH_3CN) and *trans*-stilbene (0.1 mM CH_3CN). Figure 4b shows the depletion of *trans*-stilbene from solution as (0.1 mM in CH_3CN) was monitored at 295 nm. Acenapthylene was loaded similarly and its concentration in solution was monitored at 322 nm. Again, the loading ratios were calculated by comparison of the absorbance at the plat-

eau to a Lambert-Beer plot (Supporting Information) and are summarized in Table 1. Two guests *cis*-stilbene and *trans*-β-methyl styrene did not load appreciably by method A and were instead loaded by soaking host **1** in the respective liquid guests (Method B). The complexes were air dried (6 h) and the loading was estimated by TGA (Figure 5). The small *trans*-β-methyl styrene is similar in size to coumarin and gave a similar loading ratio. In contrast, although acenaphthylene's volume (~ 170 Å^3) is close to the volume of 7-methoxy coumarin, it loaded in a higher ratio (1:0.8), perhaps due its lower polarity (2.9 D versus 7.1 D).[36,37] The loading of the stilbenes strongly favors the smaller isomer, and *cis*-stilbene was bound in a 1:1.7 host:guest ratio while the larger *trans*-stilbene was bound in a 1:0.5 host:guest ratio.

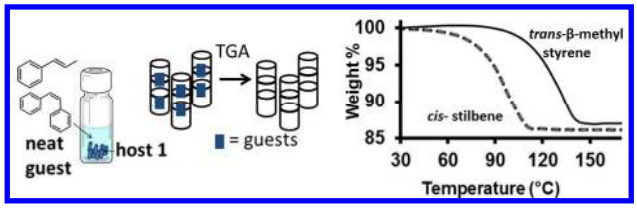

Figure 5. Formation of host•guest complexes: Schematic of loading guests via method B (left) Comparison of TGA desorption curves for host **1**•*cis*-stilbene and host **1**•*trans*-β-methyl styrene (right).

Table 1. Guests absorbed by host 1.

Guest	Dimensions (Å)	Volume (Å^3)	Polarity (D)	Host: Guest ratio
coumarin	7.6 x 3.2	147.1	5.2[a]	1:1.4[A]
6-methyl coumarin	8.2 x 3.2	167.2	5.8[a]	1:1.0[A]
7-methyl coumarin	7.7 x 3.2	167.3	5.6[a]	1:1.1[A]
7-methoxy coumarin	8.3 x 3.3	171.2	7.1[a]	1:0.5[A]
ace-naphthylene	7.1 x 3.9	170.3	2.9[b]	1:0.8[A]
trans-β-methyl styrene	8.2 x 3.3	149.9	2.3[b]	1:1.3[B]
trans-stilbene	11.6 x 3.4	215.5	2.5[b]	1:0.45[A]
cis-stilbene	8.1 x 6.2	198.7	2.9[b]	1:1.7[B]

[a]reference 36, [b]reference 37, The Host:Guest ratio superscript denotes the loading method (A or B).

In summary, host **1** appears to form stable host guest complexes with host:guest ratios ranging from 1:0.5 to nearly 1:2 for a variety of polar and/or aromatic guests with volumes that range in size from 140-220 Å^3. Two guests, 7-methoxy coumarin and *trans*-stilbene, were bound in relatively low host:guest ratios (~ 1:0.5). Next, we sought to evaluate the structures of these solid inclusion complexes using solid-state methods. The complexes were pressed to powder form and examined by powder X-ray diffraction. Figure 6a compares the PXRD patterns of host **1**•DMSO (pattern I) and the empty host **1** (pattern II) with host **1**•guests complexes. Upon removal of DMSO by TGA, the empty host **1** showed generation of new peaks at low 2θ range**.** Relative intensity of the peaks at 5.3 and 6.8 degrees were increased due to solvent removal and new peaks were observed at 9.8 and 11.7 degrees. But in the higher 2θ values (above 20 degrees) a number of peaks disappeared. These observations indicate that the host maintains crystallinity upon solvent removal. All the complexes (Figure 6a, patterns III-V) exhibit different and sharp PXRD patterns in the 2θ range of 5 to 20 degree, suggesting that each of these host **1**•guests complexes forms a different crystalline structure. The PXRD pattern of host **1**•coumarin (Figure 6a, patterns III) shows disappearance of sharp peaks at 5.3 and 6.8 degrees of the empty host **1** pattern and generation of number of peaks above 12 to 25 degrees. This result suggests after incorporating solid guest coumarin, a structural change occurred, but the complex managed to stay crystalline as a whole. Similar observations were also made for other two coumarin derivatives, 6-and 7-methyl coumarin complexes with host **1** (Figure 6a, patterns IV-V respectively). All these observations suggest incorporation of coumarin or its derivatives kept the overall material crystalline but induced changes in their overall structure due to presence of these guests. The host **1**•7-methoxy coumarin complex has the lowest host:guest ratio (~1:0.5). Its PXRD pattern showed the presence of the crystalline host and possibly the guest (Figure 6a, pattern VI). The presence of similar peaks to those of the host in the range of 5 to 20 degrees supports the existence of the crystalline host. The presence of the guest, on the other hand, appeared to be arranged in less ordered manner as indicated by the presence of new broad peak in 20 to 27 degrees.

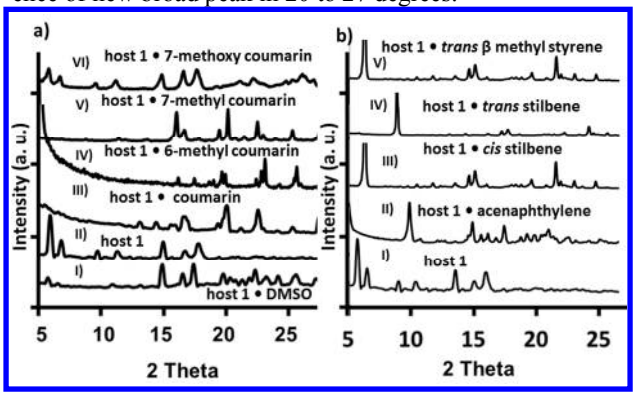

Figure 6. Comparison of the observed PXRD of host **1** and its host•guest complexes: a) Host **1** and its complexes with coumarin: I) Host **1**•DMSO, II) Host **1**, III) Host **1**•coumarin, IV) Host **1**•6-methyl coumarin, V) Host **1**•7-methyl coumarin, and IV) host **1**•7-methoxy coumarin. b) Host **1** and its complexes. I) host **1**, II) host •acenaphthylene, III) host **1**•*cis*-stilbene, IV) host **1**•*trans*-stilbene, V) host **1**•*trans*-β-methyl styrene.

In the other set of host **1**•guest complexes, similar general trends were also observed (Figure 6b, patterns II-V). The PXRD pattern of host **1**•acenaphthylene complex (Figure 6b, pattern II) showed a sharp peak at 10.2 degrees and a number of sharp peaks above 15 degrees indicating formation of a new crystalline structure. The host **1** complexes with *cis* and *trans* stilbenes (Figure 6b, pattern III and IV, respectively) showed distinct PXRD patterns. The host **1**•*cis*-stilbene complex displayed sharp peaks at 6.1, 16.6, 17.2, and 17.9 degrees 2θ. The host **1**•β methyl styrene also gives a sharp PXRD pattern that is distinct from the empty host (Figure 6b pattern V). Overall each complex displayed markedly different 2θ peaks as compared to those of the host **1**, which suggests that during the host **1**•guest complexes formation the structure of the

host **1** undergoes structural changes upon guest absorption while maintaining crystallinity. The one exception was the 7-methoxy coumarin, which loaded in the lowest ratio. Its PXRD pattern suggested that the inclusion occurs without changing the overall crystalline structure of the empty host.

The PXRD patterns probe the order and crystallinity of the complexes. To further investigate the mobility of the guests within these crystals, we turned to solid-state NMR experiments. Solid-state cross-polarized magic angle spinning $^{13}C\{^1H\}$CP-MAS (125.79 MHz) NMR spectra of solid complexes can probe the mobility of the guests. If the guests are well ordered and incorporated within the pore of the tubes, the cross-polarization behavior of the guests would be very similar to that of the host and new distinguished peaks from the guest should be observed in the spectra. Spectra I in Figure 7 shows the previously reported CP-MAS NMR of the solid empty crystals of the host **1** that shows the urea carbonyl peak at 159 ppm, aromatic region 125-140 ppm, ethynylene (sp C) peaks at 85-90 ppm and -CH- (sp^3 C) peaks at 40 ppm.[19] In comparison, the host **1**•coumarin complex (spectra II, Figure 7) displays a shift of these signature peaks of the host and/or appearance of additional peaks in the spectra. The carbons of coumarin overlap with the host in the aromatic and carbonyl regions. However, comparison of the two spectra shows the appearance of new peaks at 160-165 ppm and change in pattern at the aromatic carbonyl.

The new complexes: host **1**•6-methyl coumarin (spectra III) host **1**•7-methyl coumarin (spectra IV), and host **1**•7-methoxy coumarin (spectra V) show very similar shifting of the host resonances with little contributions from the guests, suggesting that the guests do not effectively cross-polarize probably due to their greater mobility than the host. Relatively small resonances were observed for the methyl groups in the complexes of host **1** with 6-methyl and 7-methyl coumarin between 31 - 34 ppm, Supporting Information). Similar shifts in the host were also observed in the complex with acenaphthylene (spectra VI), suggesting that all these guests have similar effects on the host structure.

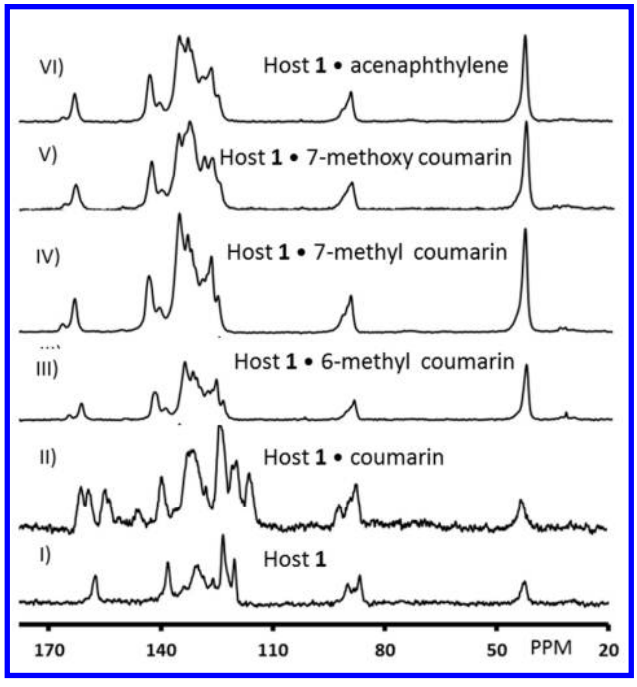

Figure 7. Comparison of solid-state $^{13}C\{^1H\}$CP-MAS NMR spectra for I) host **1**, II) host **1**•coumarin from ref 19 with the new complexes III) host **1**•6-methyl coumarin, IV) host **1**•7-methylcoumarin, V) host **1**•7-methoxy coumarin and VI) host **1**•acenaphthylene.

Solid-state characterization by PXRD and NMR indicate that the host•guest complexes are well ordered crystalline materials. Next, we wanted to investigate the effect of the encapsulation on the photoreactivity of these compounds. It is especially advantageous that the photophysical and photochemical properties of coumarin derivatives, stilbenes and *trans*-β-methyl styrene are well studied and that their respective photoproducts are readily characterized by NMR. Here, we use these potentially photoreactive guests as probes to investigate the ability of the one-dimensional channel to facilitate photochemical transformations and to influence the product distribution and selectivity.

To test the photoreactivity, a sample of each host•guest complex (30 mg) was placed in a Norell S-5-500-7 NMR tube (with 100% transmittance up to 400 nm) and UV-irradiated at room temperature under argon atmosphere using a Hanovia 450 W medium pressure mercury arc lamp. Samples (5 mg) were removed from the NMR tube after 12, 24, 96 h for analysis, and the reactions were done in triplicate. The photoproducts were isolated from the host by extraction with $CDCl_3$ and analyzed by ^1H NMR spectroscopy. Samples were also directly dissolved in DMSO-d_6 to confirm that the guests could be fully removed from the crystals. The photodimers are well studied and can be readily differentiated by their characteristic cyclobutane resonances in their ^1H NMR spectra. For acenaphthylene, coumarin, and the methylcoumarins, the conversion was estimated by comparison of the starting material to the cyclobutyl CH's. Specifically, we monitored the disappearance of the peaks that correspond to the H's attached to the reacting double bond and compared them to the newly formed cyclobutyl -CH peaks. As a control, the pure solid guests were also UV-irradiated under identical condition.

Table 2 summarizes the data from the photoreactions. First, let us compare coumarin and its derivatives. The table shows that most but not all encapsulated guest undergo reaction in the solid:host inclusion complexes. Coumarin and its derivatives undergo photolysis reactions that can potentially afford four products, although three products are mainly observed: the *syn*-HH, *syn*-HT, and *anti*-HH (Scheme 1).[38,39] We observed that host **1** facilitated the [2+2] photocycloaddition of coumarin in high selectivity for its corresponding *anti*-HH photodimer (97%, entry 3). Longer reaction times afforded an increase in conversion (entry 4-5), which is unusual as under photolysis the cycloaddition is reversible and shows limited conversion (<5%, entry 1).[40] Thus, we tested the host **1** complexes of other coumarin derivatives to see if they show similar reactivity and selectivity as host **1**•coumarin.

Scheme 1 Photolysis of Coumarin derivatives.

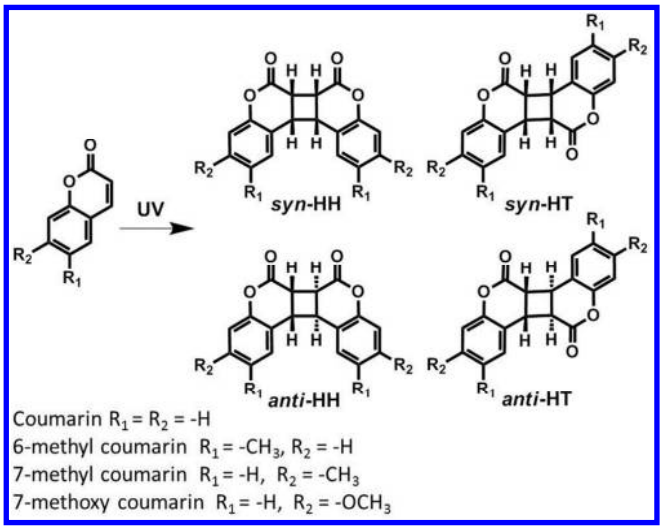

Table 2. Summary of photolysis reactions.

Guest	Entry	Host	Time h	Conv. %	Selectivity syn-HH	syn-HT	anti-HH	anti-HT
Coumarin	1	-----	96	<5	30	20	30	10
	2	Pd nanocage[a]	10	8	90	mixture of others		
	3	**1**[b]	12	19	1	0	97	1
	4	**1**[b]	24	26	1	0	97	1
	5	**1**[b]	96	55	1	0	97	1
6-methyl coumarin	6	-----	96	<5	30	20	30	10
	7	CB [8][c]	1	76	69	31	0	0
	8	**1**	12	11	14	0	84	2
	9	**1**	24	21	13	0	84	3
	10	**1**	96	46	14	0	84	2
7-methyl coumarin	11	------	96	<5	30	20	30	10
	12	CB [8][c]	12	12	>99%			
	13	**1**	12	14	2	0	97	1
	14	**1**	24	22	2	0	97	1
	15	**1**	96	51	2	0	97	1
7-methoxy coumarin	16	-----	96	12	0	>99%	----	----
	17	Pd nanocage[d]	10	55	>90%	----	----	----
	18	**1**	96	0	----	-----	----	----
						syn	*anti*	
Acenaph -thylene	19	----	96	<5		25	75	
	20	Octa acid [e]	2	24		>99		
	21	**1**	12	16		98	2	
	22	**1**	24	27		98	2	
	23	**1**	96	51		98	2	

[a]reference 49, [b]reference 19, [c]reference 43, [d]reference 49, [e]reference 54.

Upon UV-irradiation of the host **1**•6-methyl coumarin complex, we observed formation of the *anti*-HH dimer (84%) along with some of *syn*-HH dimer (14%) after 12 h in ~ 11% conversion (Table 2, entry 8). Samples of the UV-irradiated host **1**•6-methyl coumarin complex were directly dissolved in DMSO-d_6 or the guests were extracted into $CDCl_3$ and displayed new peaks that correspond to *syn*-HH dimer in the 4.0-4.1 ppm range and peaks for *anti*-HH dimer in the 3.8-3.9 ppm range (Supporting Information). Similar to coumarin, increasing the UV-irradiation time (24 h, entry 9 and 96 h, entry 10) gave an increase in conversion of 6-methyl coumarin to 21% at 24 h with 84% *anti*-HH dimer and to 46% by 96 h with similar selectivity for the *anti*-HH dimer. In comparison, UV-irradiation of solid 6-methyl coumarin showed a mixture of the four possible dimers (Table 2, entry 6) at low conversion (< 5%) due to the reversibility of this photoreaction. In solution, others observed selective photoreaction of 6-methyl coumarin in the presence of cucurbit[8]urils,[41,42,43] cyclodextrins,[44] micelles,[45,46] and complexes with optically active hosts,[47] with the *anti*-dimers postulated as originating from the triplet state.[48] A Pd nanocage[49] facilitated 15% conversion to the *syn*-HH dimer with >85% selectivity.

Similarly, UV-irradiation of host **1**•7-methyl coumarin complex also facilitated a more selective photodimerization, yielding the *anti*-HH dimer in 14% conversion in 97% selectivity after 12 h of UV-irradiation (Table 2, entry 13). Again, increased reaction time afforded an increased conversion (22% at 24 h and 51% at 96 h; entries 14 and 15) with similar high selectivity for the *anti*-HH product. The minor product (<2%) was the *syn*-HH dimer. Such high yield and selectivity was not observed upon the similar UV-irradiation of solid 7-methyl coumarin, which gave low conversion (<5%) after 96 h to afford four photodimers (Table 2, entry 11). Solid-state inclusion complexes of 7-methyl coumarin in cyclodextrin favor the *syn*-HH dimer in 99% selectivity (entry 12).[44] In solution, the conversion and selectivity depends on the polarity of the solvent, with the *anti*-HH observed in methanol.[50] Exclusive formation of the *syn*-HH dimer was observed in water with complexation by cucurbit[8]uril.[43]

We found that the host **1**•7-methoxy coumarin complex was stable to prolonged UV-irradiation (96 h). This is in contrast to what occurs in the solid 7-methoxy coumarin (entry 16), which shows low conversion (12% at 96 h) to the *syn*-HT photodimer. In solution (chloroform, methanol or water), 7-methoxy coumarin favors *syn* products (*syn*-HH and/or *syn*-HT) with >99% selectivity.[48,49]

Next, we investigated the reactivity of other complexes including acenaphthylene, *cis*- and *trans*-stilbene and *trans*-β-methyl styrene in the presence of host **1** using a similar protocol. UV-irradiation of host **1**•acenaphthylene crystals facilitated high selectivity for the *syn*-photodimer of acenaphthylene (Table 2 entry 21) in 16% conversion after 12 h. When we increase the irradiation time, we observed increased conversion (27% at 24 h and 51% at 96 h (entries 22 and 23) with similar high selectivity for the *syn* product. Acenaphthylene is known to undergo photoreactions in both solution and in the solid state. In the solid state, we observed a 1:3 ratio of *syn* and *anti* (<5% conv., entry 19). In solution, the excited singlet state of acenaphthylene undergoes [2+2] photodimerization to yield the *syn*-dimer.[51,52] In contrast, the triplet sensitized route yields both *syn* and *anti* products.[53] Ramamurthy's group investigated the use of Gibb's "octa acid" capsule in water to facilitate the photoreaction of acenaphthylene to favor the *syn*-dimer in >99% selectivity (24 % conversion, entry 20).[54] The origin of their selectivity appeared to be due to the fit of the product as the capsule could only accommodate the smaller *syn*-dimer with its dimensions of 7.2 x 6.6 Å versus the comparatively larger *anti*-dimer (6.8 x 11.8 Å).[54]

The host **1** complexes of *cis*-stilbene, *trans*-stilbene and *trans*-β-methyl styrene were all found to be stable to prolonged UV-irradiation and were recovered after 96 h of UV-irradiation time. This is similar to our controls in which no conversion was observed even after 96 h of UV-irradiation time. Crystallographic studies suggest that the photodimerization of stilbene is suppressed in the crystalline solid-state likely due to the large distance and non-parallel orientation of the olefinic double bonds of stilbenes in the crystal lattice.[55] Others have preorganized stilbenes in molecular hosts,[56,57,58,59,60] surfactant assemblies,[61] clays,[62] or employed co-crystals to organize stilbene derivatives to facilitate selective reactions.[31] Finally, *trans*-β-methyl styrene typically requires the presence of low to medium energy triplet sensitizers to undergo a photoisomerization.[33] We have observed this photoisomerization using the benzophenone containing *bis*-urea host, which contains a triplet sensitizer.[63] The lack of reactivity in host **1** sug-

gests that either this host cannot act as a sensitizer or that the guest is too constrained within the channels to undergo reaction.

Clearly, the guests within the columns displayed either reactivity or selectivity differences or both versus the controlled solids. For coumarin and its methyl derivatives, the selectivity for the *anti*-HH photodimers were very different than observed in other confined environments and these products are more typically observed in the presence of a sensitizer. For acenaphthylene, the host facilitated the reaction in similar selectivity to what is observed for Gibbs Octa-acid, a selectivity whose origin is likely guided by a favorable fit of the *syn*-product within the confined space.[54] Our hypothesis is that the origin of both the different reactivity and the selectivity of these reactions within their host **1** complexes is due to the confinement of the guests within the confined one-dimensional channel of host **1**. To test this hypothesis, we turned to molecular simulations.

The earlier simulations of the host **1**•coumarin complexes were done using Spartan[64] by importing the atomic coordinates from the host **1**•nitrobenzene crystal structure and deleting the guests. In those calculations, a truncated column of 4 macrocycles was 'frozen' and guests were added sequentially and minimized until additional guests were ejected during the minimization process. Monte Carlo searching of the conformer distributions at the ground state with molecular mechanics (MMFF) afforded 450 conformers. From analysis of the ten lowest energy conformers, we concluded that 1) the guests were paired in close proximity within the distance (< 4.2 Å) required for the [2+2] photocycloaddition, 2) the guests have room to move relative to their neighbors and to the channel framework, and 3) the guests do not appear to be preorganized to favor only one photodimer selectively. Disadvantages of this calculation include intensive computational time, truncated model (only 4 macrocycles were used), and observations of some distortion of the urea hydrogen bond motif. Our experimental data suggests that the structure of the columns do not change significantly structure during guest absorption, subsequent guest reaction and product removal. Therefore, we sought to reexamine our system using additional GCMC simulations.

We investigated methods to apply Monte Carlo for Complex Chemical Systems (MCCCS) Towhee plug-in built into Scienomics' Materials Processes and Simulations (MAPS) platform. The direct modeling of a single column, analogous to the prior procedure, did not produce columns with paired guests. Instead, a new procedure was required. The simulation cell (Figure 8a) was generated by importing the atomic coordinates from the single crystal X-ray structure of host **1**•nitrobenzene and omitting the coordinates of the guest atoms. The GCMC simulation on the crystalline host **1**•coumarin complex was conducted for $1x10^6$ steps. We analyzed significant configurations of these simulations to probe the movement/mobility and orientation of the guest molecules within the simulation cell. A brief movie was compiled to show the movement of coumarin molecules inside the channel during the simulation by capturing last 11 simulation frames (ESI).

Figure 8b, shows the coumarins load into the columns and pair together, similar to the earlier Spartan predictions. The two coumarins interact through aryl stacking interactions (Figure 2b) and the reacting alkenes are in close proximity (4 Å), although not optimally aligned. Both simulations show the coumarins closely paired; however, the alignment in the MAPS simulation suggests that they are preorganized to favor formation of an *anti*-HH dimer product (Figure 8c). Interestingly, the simulation also predicted that some coumarin guests load in between the neighboring columns (Fig. 8b), much like alcohol guests in our pyridyl systems;[65] however, these coumarins are not paired and are spaced at distances and geometries that are unfavorable for reactions. This exterior loading may arise from the way the simulation cell has been constructed (Fig. 8a), although we have no experimental data to suggest that guests are loaded in such exterior binding sites.

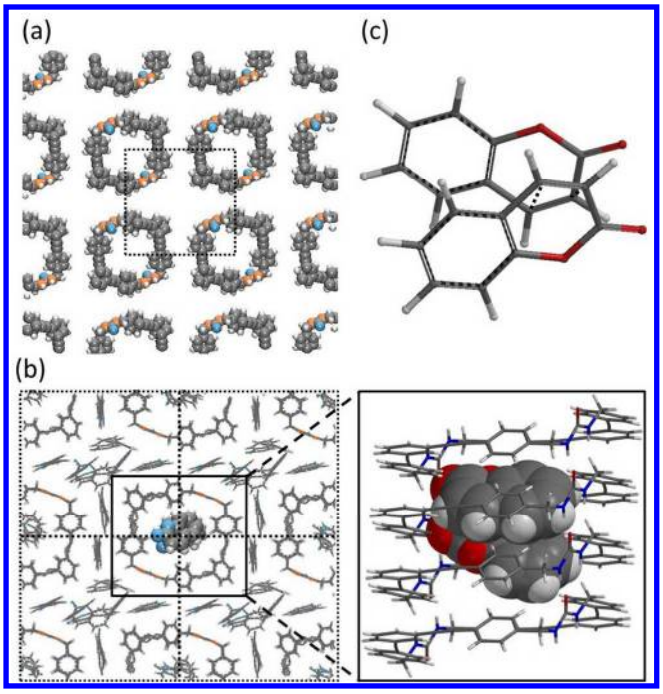

Figure 8. GCMC simulations for the host **1**•coumarin complex. a) The periodic simulation cell used for GCMC simulations. b) Simulations indicate coumarin guests are paired in the channel (shown in space filling models). Simulations also suggest that guests may fit in between columns, although no close contacts were predicted between the reactive alkenes. c) Orientation of two coumarin molecules paired in the channel.

We next applied this same method to analyze other guests. Watching the simulation frames from the loading of 6-methyl coumarin, we observed two molecules of 6-methyl coumarin enter the simulation cell, move towards the center and pair together even before reaching to the step number $1x10^5$. The two guests rapidly orient themselves in the *anti* orientation to each other where their carbonyl head groups are pointing to the same direction (Figure 9a). This pairing is stabilized by CH-π (Figure 2c) and aryl stacking interactions between the guests and the channel walls. The paired coumarins also interact by aryl stacking interactions (3.4 Å) and remain close together throughout the remaining simulation. In the minimized structure, the paired 6-methyl coumarins are offset from each other by 1.4 Å, and the olefinic double bonds are located approximately 4.0 Å apart. Although the reactive double bonds are organized at a favorable distance, they are not in the optimal parallel alignment. Others have observed the [2+2] photodimerization from non-parallel orientations in the solid-state.[66,67] Given the orientation in Figure 9a, there is a high probability that the photodimerization will afford the *anti*-HH dimer, which is in agreement with the experimental results.

After the reactants are paired in the center column, we focused on what the other molecules do in the extended system, keeping in mind that the rest of the simulation cell shows the edges of the columns or partial columns. The next two molecules enter into the host macrocycle from opposite ends of the simulation cell and have no pair within the simulation cell. Throughout the simulation the stand-alone 6-methyl coumarin molecules are on the edges of our simulated cell, where they have the ability to rotate and adopt a number of configurations, a pattern that emerges in subsequent calculations. This indicates not all the guest molecules that are absorbed by the host are present in an orientation to form dimers, and the yield of dimer forming reaction is expected to be lower. This could account for the observed conversion limit of ~ 50% even after 96 h of photoirradiation; however, other facts such as inefficient light penetration or non-uniform UV-irradiation could also play a role. Taken together, the simulation suggests that there is room within the host macrocycle for the 6-methyl coumarin molecules to rotate and change between configurations until two neighboring 6-methyl coumarins are paired, which fixes them in a configuration that favors *anti*-HH dimer formation.

A similar approach was used to investigate the 7-methyl coumarin guests, which is similar in dimension to its isomer 6-methyl coumarin (table 1). Here, again we observe a fast pairing of two guests in the central channel, which occurs within the first $1x10^5$ steps. After minimization (Figure 9b), the pairs are located 3.2 Å away from each other and offset from each other in the by 3.0 Å with their olefinic double bond is located 3.8 Å apart, although they are not exactly aligned and suprafacial for the subsequent photoreaction. While some movement is required for a dimerization to occur, the two closely paired molecules are preorganized to primarily product the *anti*-HH photodimer, which is experimentally observed with 97% selectivity.

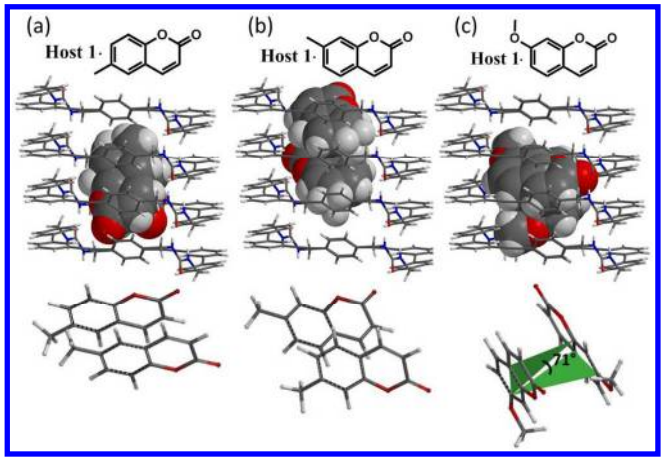

Figure 9. GCMC simulation results for coumarin derivatives. (Partial guest molecules omitted for clarity). a) Orientation of 6-methyl coumarin molecules inside the channel of host **1**. b) Orientation of 7-methyl coumarin molecules inside the channel. c) Orientation of 7-methoxy coumarin molecules inside the channel.

The same procedure was used to analyze the unreactive host **1**•7-methoxy coumarin complex. This coumarin derivative was the largest and most polar tested (table 1) and was absorbed in the lowest ratio (1:0.5). The simulations suggest that each 7-methoxy coumarin guest interacts with the walls of the channel through edge to face aryl stacking interactions (Figure 9c). The distance from the aryl H of the phenyl rings on the host to the center of the aryl ring of the coumarin guests range is ~ 2.7 Å. Two neighboring coumarins approach each other but are not as closely paired as in the previous examples. The planes of the neighboring coumarins are rotated 71.3° with respect to each other and the closest approach is 3.7 Å (plane to plane). Simulation results after $1x10^6$ steps showed the olefinic double bonds of two molecules located ~5.7 Å apart. This suggests that the two guest molecules are not oriented to favor the dimer formation, which was also observed experimentally.

Acenaphthylene is slightly larger than the methylcoumarins (170 $Å^3$ versus 167 $Å^3$) and is bound in an ~ 1:1 host:guest ratio. The simulation of host **1**•acenapthylene suggests thee acenaphthylenes will be quickly bound in the central channel of our periodic cell (Figure 10a). Two are close packed and the third is at the end of the simulated tube roughly perpendicular and interacts with its neighbor through edge to face aryl-stacking interactions. This perpendicular orientation is not preorganized for reaction and may be a contributing factor in the observed moderate conversion (51%). Additional insight was obtained by analyzing the compiled 'snapshots' over course of the minimization. During the minimization process, it appears that the perpendicular acenapthylene is frequently observed often before its neighbor's bind and may provide additional contacts for organizing the pair. Closer inspection of this pair shows they are oriented in a configuration that should favor the *syn*-photodimer, which is the experimentally observed product.

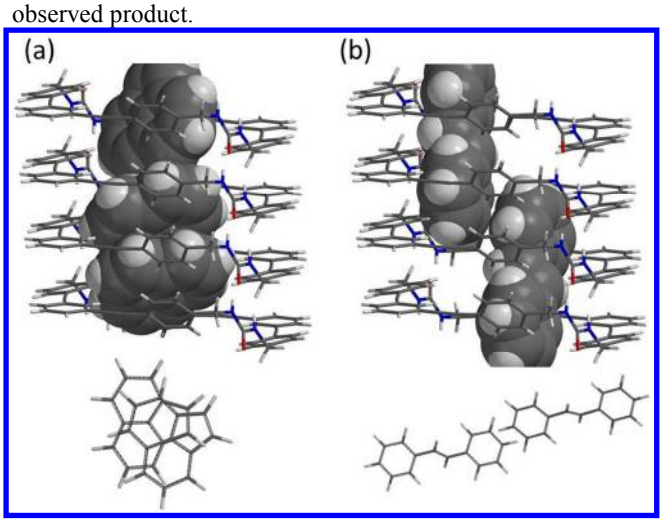

Figure 10. GCMC simulation results of host **1**•acenaphthylene and host **1**•*trans*-stilbene. (Partial guest molecules omitted for clarity.) a) Predicted orientation of acenaphthylene molecules inside the channel of host **1**. b) Orientation of *trans*-stilbene molecules inside the channel.

GCMC simulations of the host **1** complexes with *cis*-stilbene, *trans*-stilbenes (Figure 10b) and β-methyl styrene predicted these guests are randomly distributed within the tubes with limited close contacts with neighboring guests. Similar to the models of the host **1**•coumarin, some loading of these guests was also predicted to occur in an exterior binding site between neighboring tubes. These exterior absorbed guests also lacked proximity to neighboring guests and displayed geometries that were not conducive for further reaction.

Summary and conclusions

This manuscript demonstrates the utility of our self-assembled phenylethynylene *bis*-urea host to absorb a range of

aromatic guests and form well-ordered crystalline complexes as indicated by PXRD. Subsequent solid-state $^{13}C\{^{1}H\}$CP-MAS NMR studies suggest that the encapsulated guests have a greater mobility within the solid than the assembled host. The guests were chosen based on their propensity to undergo photochemical reactions and were used to probe the ability of the one-dimensional channel to influence or direct photochemical transformations. Upon UV-irradiation, we observed selective photodimerization reactions for coumarin, 6-methyl coumarin, and 7-methyl coumarin to afford their corresponding *anti*-HH photodimers with good to excellent selectivity (84-97%) in moderate conversion. Acenaphthylene also reacted selectively in the solid host **1**•acenaphthylene complex to afford exclusive production of the syn-photodimer. Not all the guests reacted in the presence of host **1**. No isomerization reactions were observed for the *cis*-stilbene, *trans*-stilbene, or *trans*-β-methylstyrene complexes, which indicates that host **1** is not able to act as a sensitizer. Also, no [2+2]-photocycloadditions were observed for these guests, suggesting that either they were bound in geometries that were not conducive for reactions or that the photoproducts were too large for the channel.

The most important aspect of this manuscript was the development of a protocol to examine these host guest complexes by GCMC simulations. These were carried out with Monte Carlo for Complex Chemical Systems (MCCCS) Towhee plug-in built into Scienomics' MAPS. The simulations were not only able to explain the observed reactivity of these guests, but also correctly predicted the product selectivity. Indeed, in the simulations the reactive guests (coumarin, 6-methyl coumarin, 7-methyl coumarin and acenaphthylenes) appeared to be closely paired within the channels and were preorganized with respect to each other to most easily form their respective *anti*-HH or *syn* photodimers. These were also the experimentally observed products. Thus, our simulations suggest that the selectivity is due to the pre-organization of the starting materials within the channels of host **1.**

Our simulations also predicted that there could potentially be loading of guests in sites on the exterior in between neighboring one-dimensional columns, although these guests were positioned in geometries and at distances that were unfavorable for subsequent reactions. Thus far, we have no experimental evidence of such binding modes; however, such binding could provide an alternative explanation for the apparent conversion limit of ~55%. This limit could also due to inefficient light penetration or lack of uniform irradiation of the crystals. Currently, collaborators C. Russ Bowers and Sergey Vasenkov are exploring molecular transport processes within host **1** through pulsed field gradient NMR and hyperpolarized Xenon-129 tracer exchange experiments and we hope to report on these results soon. We are currently working to refine these simulations and are applying this method to more broadly to predict the loading and potential reactive of new guests within this porous host. We expect this synergy between experiment and simulations to guide our future studies.

ASSOCIATED CONTENT

Supporting Information. ^{1}H-NMR and ^{13}C-NMR spectra, loading data and Beer-Lambert plots, powder X-ray diffraction (PXRD), thermogravimetric analysis and simulation details. This material is available free of charge via the Internet at http://pubs.acs.org.

AUTHOR INFORMATION

Corresponding Author

*shimizls@mailbox.sc.edu

Author Contributions

[#]These authors contributed equally to the experiments and paper authorship. The manuscript was written through contributions of all authors. / All authors have given approval to the final version of the manuscript.

[+]Current address for ACW: Department of Chemistry, Faculty of Science, University of Malaya, Kuala Lumpur, 50603, Malaysia.

Funding Sources

NSF (CHE-1305136)

ACKNOWLEDGMENT

The authors gratefully acknowledge support for this work from the NSF (CHE-1305136).

ABBREVIATIONS

PXRD, powder X-ray diffraction; TGA, thermogravimetric analysis; NMR, Nuclear Magnetic Resonance; DMSO, dimethyl sulfoxide.

REFERENCES

[1] Yoshizawa, M.; Klosterman, J. K.; Fujita, M. Functional molecular flasks: New properties and reactions within discrete, self-assembled hosts. *Angew. Chem., Int. ed.* **2009**, *48*, 3418-3438.

[2] Breiner, B.; Clegg, J. K.; Nitschke, J. R. Reactivity modulation in container molecules. *Chem. Sci.* **2011**, *2*, 51-56.

[3] Vriezema, D. M.; Aragones, M. C.; Ellemans, J. A. A. W.; Cornelissen, J. J. L. M.; Rowan, A. E.; Nolte, R. J. M. Self-assembled nanoreactors. *Chem. Rev.* **2005**, *105*, 1445-1489.

[4] Pluth, M. D.; Bergman, R. G.; Raymond, K. N. Acid catalysis in basic solution: A supramolecular host promotes orthoformate hydrolysis. *Science* **2007**, *316*, 85-87.

[5] Fiedler, D.; Bergman, R. G.; Raymond, K. N. Supramolecular catalysis of a unimolecular transformation: Aza-cope rearrangement within a self-assembled host. *Angew. Chem., Int. ed.* **2004**, *43*, 6748-6751.

[6] Murase, T.; Horiuchi, S.; Fujita, M. Naphthalene diels-alder in a self-assembled molecular flask. *J. Am. Chem. Soc.* **2010**, *132*, 2866-2867.

[7] Yoshizawa, M.; Tamura, M.; Fujita, M. Diels-alder in aqueous molecular hosts: Unusual regioselectivity and efficient catalysis. *Science*, **2006**, *312*, 251-255.

[8] Frei, H. Selective hydrocarbon oxidation in zeolites. *Science*, **2006**, *313*, 309-310.

[9] Yumura, T.; Takeuchi, M.; Kobayashi, H.; Kuroda, Y. Effects of ZSM-5 zeolite confinement on reaction intermediates during dioxygen activation by enclosed dicopper cations. *Inorg. Chem.* **2009**, *48*, 2, 508-519.

[10] Yoshizawa, M.; Takeyama, Y.; Kusukawa, T.; Fujita, M. Cavity-directed, highly stereoselective [2+2] photodimerization of olefins within self-assembled coordination cages. *Angew. Chem., Int. Ed.* **2002**, *21*, 1347-1349.

[11] Yang, J.; Dewal, M. B.; Profeta, S.; Smith, M. D.; Li, Y.; Shimizu, L. S. Origins of selectivity for the [2+2] cycloaddition of α,β-unsaturated ketones within a porous self-assembled organic framework. *J. Am. Chem. Soc.* **2008**, *130*, 612-621.

[12] Raymond, K. N. Supramolecular Chemistry: Phosphorus caged. *Nature* **2009**, *460*, 585-586.

[13] Ramamurthy, V.; Caspar, J. V.; Corbin, D. R. Modification of photochemical reactivity by zeolites – Generation, entrapment, and

spectroscopic characterization of radical cations of alpha, omega-diphenyl polyenes within the channels of pentasil zeolites. *J. Am. Chem. Soc.* **1991**, *113*, 594-600.

[14] Ziegler, M.; Brugmaghim, J. L.; Raymond, K. N. Stabilization of a reactive cationic species by supramolecular encapsulation. *Angew. Chem., Int. ed.* **2000**, *39*, 4119-4121.

[15] Iwasawa, T.; Hooley, R. J.; Rebek, J. Stabilization of labile carbonyl addition intermediates by a synthetic receptor. *Science*, **2007**, *317*, 493-497.

[16] Rao, V. J.; Prevost, N.; Ramamurthy, V.; Kojima, M.; Johnston, L. J. Generation of stable and persistent carbocations from 4-vinylanisole within zeolites. *Chem. Commun.* **1997**, 2209-2210.

[17] Lambert, J. B. Chemistry a tamed reactive intermediate. *Science*, **2008**, *322*, 1333-1334.

[18] Koblenz, T. S.; Wassenaar, J.; Reek, J. N. H. Reactivity within a confined self-assembled nanospace. *Chem. Soc. Rev.* **2008**, *37*, 247-262.

[19] Dawn, S.; Dewal, M. B.; Sobransingh, D.; Paderes, M. C.; Wibowo, A. C.; Smith, M. D.; Krause, J. A.; Pellechia, P. J.; Shimizu, L. S. Porous crystals from self-assembled phenylethynylene *bis*-urea macrocycles facilitate the selective photodimerization of coumarin. *J. Am. Chem. Soc.* **2011**, *133*, 7025-7032.

[20] Ramamurthy, V.; Parthasarathy, A. Chemistry in restricted spaces: Select photodimerizations in cages, cavities and capsules. *Isr. J. Chem.* **2011**, *51*, 817-829.

[21] Ginsberg, D.; Schmidt, G. M. J. Solid State Photochemistry, Verlag Chemie, New York, 1976.

[22] Cohen, M. D. Photochemistry of organic solids. *Angew. Chem. Int. Ed. Engl.* **1975**, *14*, 386-393.

[23] Weiss, R. G.; Ramamurthy, V.; Hammond, G. S. Photochemistry in organized and confining media – A model. *Acc. Chem. Res.* **1993**, *26*, 530-536.

[24] Qiu, Y.; Kaifer, A. E. Reactivity of redox-active guests trapped inside molecular capsules. *Isr. J. Chem.* **2011**, *51*, 830-839.

[25] Purse, B. W.; Rebek, J. Functional cavitands: Chemical reactivity in structure environments. *P. Natl. Acad. Sci. USA* **2005**, *102*, 10777-10782.

[26] Kim, K.; Selvapalam, N.; Ko, Y. H.; Park, K. M.; Kim, D.; Kim, J. Functionalized cucurbiturils and their applications. *Chem. Soc. Rev.* **2007**, *36*, 267-270.

[27] Ajami, D.; Rebek, J. More chemistry in small spaces. *Acc. Chem. Res.* **2013**, *46*, 990-999.

[28] Gibb, C. L. D.; Gibb, B. C. Well-defined, organic nanoenvironments in water: The hydrophobic effects drives a capsular assembly. *J. Am. Chem. Soc.* **2004**, *126*, 11408-11409.

[29] Zhang, Y.; Riduan, S. N. Functional porous organic polymers for heterogeneous catalysis. *Chem. Soc. Rev.* **2012**, *41*, 2083-2094.

[30] Organic Solid State Reactions, Topics in Current Chemistry; Toda, F., Ed.; Springer-Verlag: Berlin, 2005; Vol. 254.

[31] MacGillivray, L. R.; Papaefstathiou, G. S.; Friscic, T.; Hamilton, T. D.; Bucar, D. K.; Chu, Q.; Varshney, D. B.; Georgiev, I. G. Supramolecular control of reactivity in the solid state: From templates to ladderanes to metal-organic frameworks. *Acc. Chem. Res.* **2008**, *41*, 280-291.

[32] Materials and Processes Simulations (MAPS), Copyright Scienomics SARL, Paris, France, 2004-2013.

[33] Arai, T.; Sakuragi, H.; Tokumaru, K. Photosensitized *cis-trans* isomerization of beta-alkylstyrenes. *Bull. Chem. Soc. Jpn.* **1982**, *55*, 2204-2207.

[34] Mayo, S. L.; Olafson, B. D.; Goddard, W. A. Dreiding: A generic force field for molecular simulations. *J. Phys. Chem.* **1990**, *94*, 8897-8909.

[35] Kamlet, M. J.; Abboud, J. L.; Taft, R. W. Solvatochromic comparison method. 6. The Pi-* scale of solvent polarities. *J. Am. Chem. Soc.* **1977**, *99*, 6027-6038.

[36] Pandey, N.; Gahlaut, R.; Arora, P.; Joshi, N. K.; Joshi, H. C. Study of dipole moments of some cumarin derivatives. *J. Mol. Structure* **2014**, *1061*, 175-180.

[37] Everard, K. B.; Kumar, L.; Sutton, L. E. Polarisation in conjugated systems. Part 1. The refractions and electric dipole moments of some derivatives of benzene, styrene, diphenyl, stilbene, and 1,4 biphenyl butadiene. *J. Chem. Soc.* **1951**, 2807-2851.

[38] Krauch, H.; Farid, S.; Schenck, G. O. Photo-C4-cyclodimerisation von coumarin. *Chem. Ber.* **1966**, *99*, 625-631.

[39] Hoffman, R.; Wells, P.; Morrision, H. Organic photochemistry. 12. Further studies on mechanism of coumarin photodimerization – observation of an unusual heavy atom effect. *J. Org. Chem.* **1971**, *36*, 102-107.

[40] Tanaka, K.; Toda, F. Solvent-free organic synthesis. *Chem. Rev.* **2000**, *100*, 1025-1074.

[41] Pemberton, B. C.; Barooah, N.; Srivatsava, D. K.; Sivaguru, J. Supramolecular photocatalysis by confinement-photodimerization of coumarins within cucurbit[8]urils. *Chem. Commun.* **2010**, *46*, 225-227.

[42] Pemberton, B. C.; Singh, R. K.; Johnson, A. C.; Jockusch, S.; Da Silva, J. P.; Ugrinov, A.; Turro, N. J.; Srivastava, D. K.; Sivaguru, J. Supramolecular photocatalysis: insights into cucurbit[8]urils catalyzed photodimerizationof 6-methylcoumarin. *Chem. Commun.* **2011**, *47*, 6323-6325.

[43] Barooah, N.; Pemberton, B. C.; Johnson, A. C.; Sivaguru, J. Photodimerization and complexation dynamics of coumarins in the presence of cucurbit[8]urils. *Photoch. Photobio. Sci.* **2008**, *7*, 1473-1479.

[44] Moorthy, J. N.; Venkatesan, K.; Weiss, R. G. Photodimerization of coumarins in solid cyclodextrin inclusion complexes. *J. Org. Chem.* **1992**, *57*, 3292-3297.

[45] Yu, X. L.; Scheller, D.; Rademacher, O.; Wolff, T. Selectivity in the photodimerization of 6-alkylcoumarins. *J. Org. Chem.* **2003**, *68*, 7386-7399.

[46] Muthuramu, K.; Ramamurthy, V. Photodimerization of coumarin in aqueous and micellar media. *J. Org. Chem.* **1982**, *47*, 3976-3979.

[47] Tanaka, K.; Fujiwara, T. Enantioselective [2+2]-photodimerization reactions of coumarins in solution. *Org. Lett.* **2005**, *7*, 1501-1503.

[48] Wolff, T.; Gorner, H. Photodimerization of coumarin revisited: Effects of solvent polarity on the triplet reactivity and product pattern. *Phys. Chem. Chem. Phys.* **2004**, *6*, 368-376.

[49] Karthikeyan, S.; Ramamurthy, V. Templating photodimerization of coumarins within a water-soluble nano reaction vessel. *J. Org. Chem.* **2006**, *71*, 6409-6413.

[50] Haga, N.; Takayanagi, H.; Tokumaru, K. Mechanism of photodimerization of acenaphthylene. *J. Org. Chem.* **1997**, *62*, 3734-3743.

[51] Cowan D. O.; Drisko, R. L. E. Photochemical Reactions. 4. Photodimerization of acenaphthylene – Mechanistic studies. *J. Am. Chem. Soc.* **1970**, *92*, 6286-6291.

[52] Nerbonne, J. M.; Weiss, R. G. Liquid crystalline solvents as mechanistic probes. 3. The influence of ordered media on the efficiency of the photodimerization of acenaphthylene. *J. Am. Chem. Soc.* **1979**, *101*, 402-407.

[53] N. J. Turro, Cycloaddition reactions; Modern Molecular Photochemistry, University Science books: Sausalito, CA, 1991; 462-464.

[54] Kaanumalle, L. S.; Ramamurthy, V. Photodimerization of acenaphthylene within a nanocapsule: Excited state lifetime dependent dimer selectivity. *Chem. Commun.* **2007**, 1062-1064.

[55] Rao, K. S. S. P.; Hubig, S. M.; Moorthy, J. N.; Kochi, J. K. Stereoselective photodimerization of (E)-stilbene in crystalline gamma-cyclodectrin inclusion complexes. *J. Org. Chem.* **1999**, *64*, 8098-8104.

[56] Ohara, K.; Inokuma, Y.; Fujita, M. The catalytic Z to E isomerization of stilbenes in a photosensitizing porous coordination network. *Angew. Chem., Int. Ed.* **2010**, *49*, 5507-5509.
[57] Parthasarathy, A. Ramamurthy, V. Role of free space and weak interactions on geometric isomerization of stilbenes held in a molecular container. *Photochem. Photobiol. Sci.* **2011**, *10*, 1455-1462.
[58] Dube, H.; Ams, M. R.; Rebek, J. Supramolecular control of fluorescence through reversible encapsulation. *J. Am. Chem. Soc.* **2010**, *132,* 9984-9985.
[59] Choi, S.; Park, S. H.; Ziganshina, A. Y.; Ko, Y. H.; Lee, J. W.; Kim, K. A stable *cis*-stilbene derivative encapsulated in cucurbit[7]uril. *Chem. Commun.* **2003**, 2176-2177.
[60] Duveneck, G. L.; Sitzmann, E. V.; Eisenthal, K. B.; Turro, N. J. Picosecond laser studies on photochemical reactions in restricted environments – The photoisomerization of trans-stilbene complexed to cyclodextrins. J. *Phys. Chem.* **1989**, *93*, 7166-7170.
[61] Whitten, D. G. Photochemistry and photophysics of *trans*-stilbene and related alkenes in surfactant assemblies. *Acc. Chem. Res.* **1993**, *26*, 502-509.
[62] Madhavan, D.; Pitchumani, K. Photodimerisation of acenaphthylene in a clay microenvironment. *Photochem. Photobiol. Sci.*, **2003**, *2*, 95-97.
[63] Dewal, M. B.; Xu, Y.; Yang, J.; Mohammed, F.; Smith, M. D.; Shimizu, L. S. Manipulating the cavity of a porous material changes the photoreactivity of included guests. *Chem. Commun.* **2008**, 3909-3911.
[64] Spartan 04 for Macintosh, V. 1.1.1.; Wavefunction, Inc.: Irvine, CA, 2007.
[65] Roy, K.; Wang, C.; Smith, M. D.; Dewal, M. B.; Wibowo, A. C.; Brown, J. C.; Ma, S.; Shimizu, L. S. Guest induced transformations of assembled pyridyl *bis*-urea macrocycles. *Chem. Commun.* **2011**, *47*, 277-279.
[66] Murthy, G. S.; Arjunan, P.; Venkatesan, K.; Ramamurthy, V. Consequences of lattice relaxability in solid-state photodimerizations. *Tetrahedron* **1987**, *43*, 1225-1240.
[67] Bhadbhade, M. M.; Murthy, G. S.; Venkatesan, K.; Ramamurthy, V. Topochemical dimerization of non-parallel double-bonds – 7-methoxycoumarin. *Chem. Phys. Lett.* **1984**, *109*, 259-263.

For Table of Contents Use Only